www.czasopisma.pan.pl PAN POLSKA AKADEMIA NAUK www.journals.pan.pl

Arch. Min. Sci. **65** (2020), 1, 179-194

Electronic version (in color) of this paper is available: http://mining.archives.pl

DOI 10.24425/ams.2020.132714

TUO WANG[1], JUCAI CHANG[2*], PENG GONG[1],WENBAO SHI[2],
NING LI[1], SHIXING CHENG[1]

THE EXPERIMENTAL INSTRUMENTED BOLT WITH FIBRE BRAGG GRATING FORCE SENSORS

Monitoring the stress change of bolt and knowing the anchoring condition in a reasonable and effective way, accurately, can effectively prevent tunnel accident from breaking out. The stress of rock mass around the roadway is usually transferred to the anchor rod in the form of axial load, so it is of great significance to study the axial load of the bolt. In this paper, a full size anchoring and drawing experiment system was designed and established, innovatively, which realized the pull-out test of 2.5 m prestressed end Anchorage and the full-length Anchorage by using the new resin anchorage agent under vertical and horizontal loads. Through the application of fiber Bragg grating (FBG) sensing technology to the test of full-scale anchor rod, the axial force distribution characteristics of the end Anchorage and the full-length Anchorage anchor rod were obtained under the action of pre-tightening torque and confining rock pressure. The comparison indicates that the proportion of high stress range accounts for only 17.5% and the main bearing range is near the thread end of anchor rod, the proportion of main bearing range of end Anchorage is 83.3%, and the feasibility of FBG force-measuring anchor rod is verified in the field. The research results have certain reference value.

Keywords: Fiber Bragg Grating, pullout test, Anchorage system, pre-tightening torque, Bolt Support

1. Introduction

Bolt support is active support, which can strengthen the structure of surrounding rock, improve the stability and integrity of surrounding rock of roadway, and is convenient for construction, and can support in time and effectively (Stillborg, 1986; Kang Hongpu, 2010; Chen, 2016,

[1] CHINA UNIVERSITY OF MINING AND TECHNOLOGY, STATE KEY LABORATORY FOR GEOMECHANICS AND DEEP UNDERGROUND ENGINEERING, XUZHOU 221116, CHINA
[2] ANHUI UNIVERSITY OF SCIENCE AND TECHNOLOGY, SCHOOL OF ENERGY AND SAFETY ENGINEERING, KEY LABORATORY OF SAFETY AND HIGH-EFFICIENCY COAL MINING, MINISTRY OF EDUCATION

* Corresponding author: cjcminecoal@163.com

2017), and reinforce rock mass by restraining the deformation around the roadway. At present, bolt support technology has been widely used at home and abroad, is one of the key technologies to achieve high production and high efficiency in coal mines (Windsor, 1993; Wang Tuo, 2016; Cai, 2004; Li, 2007; Li, 2016). The use of bolt in the whole world exceeds 500 million according to (Hillyer, 2012). The roadway bolt support rate in China's large and medium-sized state-owned coal mines is over 60%, and in some mining areas more than 90% or even up to 100%.

China is the world's largest coal consumer, with total energy consumption of 4.49 billion tons of standard coal in 2017, an increase of 2.9% over the previous year, coal consumption accounted for 60.4% of the total energy consumption, calculated in absolute terms. Coal consumption in 2017 increased by 0.4% from the same period last year. The million-ton mortality rate of coal mines dropped from 2.76 in 2005 to 0.106 in 2017. However, coal mine production in China is still a high-risk industry with frequent mining accidents, and there is still a big gap compared with the developed countries in the world. The death rate of one million tons is five times that of the United States, eleven times that of Australia. In all of these accidents, roof accidents accounted for 51.22% of all kinds of accidents in China on average, which is much higher than that of other major coal-producing countries in the world. Therefore, using reasonable and effective means to monitor the stress and strain of roadway support is an important way to prevent roof accidents.

Pre-tightening force is an important parameter in the design of bolting support. It can improve the stress state of surrounding rock of roadway and limit the expansion of rock mass. (Gao & Kang, 2008; Kang et al., 2009) have found that for this type of rock anchor, when a high pretension (pretension) (30-50% yield load) is installed, the roadway deformation and failure are greatly suppressed. Due to the complexity of construction technology (Chen, 2016), it is usually difficult to apply pre-tightening force to the anchor rod, and most of the full-length anchoring bolts are difficult to apply pre-tightening force (Li Chong, 2013), the main reason is that the anchoring agent solidifies too fast. Stillborg (1984) used concrete materials to cast cylindrical samples with a diameter of 300 mm and conducted pull-out tests on plain cable bolts. His results showed that the greasy substance coated on plain cable bolts had a negative effect on the bonding capacity of cable bolts and recommended that the cable bolt surface should be kept clean before installation. Benmokrane et al. (1995) conducted pull-out tests on plain cable bolts installed in samples with a diameter of 200 mm, finding that the cable surface geometry and grout had a significant effect on the bonding capacity of cable bolts, especially when large displacement occurred. Z.J. Yang (2010) proposed an analytical solution for predicting the full-range mechanical behaviour of grouted rockbolts in tension. The whole process was divided into five consecutive stages and the ultimate load and effective anchoring length of anchor rod were calculated. The analytical model was calibrated and verified by two pull-out experiments. The end Anchorage is used in the roadway with high ground stress, the bolt body is subjected to high stress range, and the bolt is prone to break down and hurt. The full-length anchoring also has certain restriction on this situation. The failure forms of bolt in roadway mainly include free end breakage and anchor slip failure, all of which can be improved by full-length anchoring. Two kinds of bolt failure forms are shown in Figure 1.

FBG is characterized by high measurement accuracy, good stability and long transmission distance. At present, FBGs have been widely used in civil engineering, water conservancy engineering, aerospace and other fields, and have achieved remarkable results. H.J. Patrick (2000) solved the cross-sensitivity problem between temperature and strain by using the combination

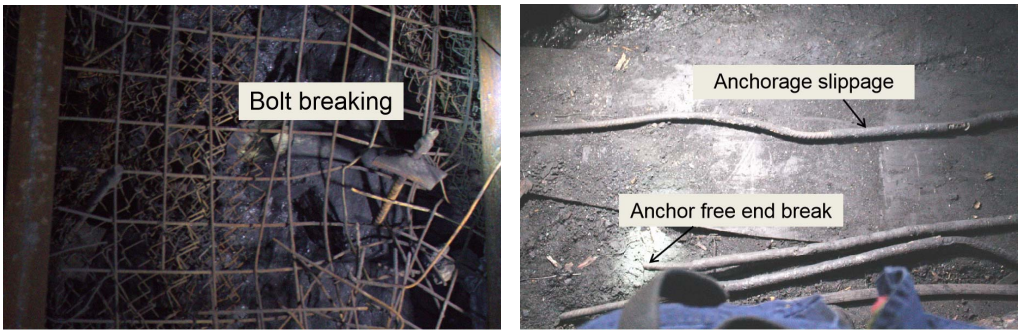

(a) (b)

Fig. 1. Anchorage Failure. (a) Anchor slippage at high stress; (b) Anchorage end slip and free end break

of long-period fiber grating and fiber Bragg grating, and realized the simultaneous measurement of temperature and strain. López-Higuera J.M. (2011) also discussed several examples of the use of OFS in practical structures, including examples from the renewable energy, transport, civil engineering and oil and gas industries, as well as some of the challenges to be faced in the near future. Wolfgang R. Habel (2011) introduces a special fiber optic chemical sensor used to monitor the basic state of cement matrix (pH) in reinforced concrete structure, and a FBG sensor connected to anchoring steel (micro-pile) to measure the strain distribution in the loaded earth anchor. In recent years, the application of FBG sensor in bolt monitoring is also in the stage of research and development, and a lot of progress has been made. Chai Jing (2012, 2014) using FBG to detect the strain of anchor rod in the experiment, using Gao Si function to fit the measured data of strain on bolt body, the distribution of axial force and shear force of anchor rod is obtained. Forbes (2017) considers monitoring three sensing lengths along the profile of a fully grouted rock bolt element using a single optical fiber, which shows the potential of this technique to capture the characteristics of anchor under the condition of generalized anchor loading. Nicholas Vlachopoulos (2018) makes use of a new distributed optical strain sensing technique to capture the strain along the anchor rod and study the influence of the variation of these parameters on the mechanical response of steel bars under axial loading with different embedding lengths and borehole diameters.

The stress experienced by rock mass is usually transmitted to the anchor rod in the form of axial load. It is of great significance to study the axial load transfer of the anchor rod. At present, most of the research on bolt mechanics is in the range of small size, and the surrounding rock of anchor body is tested without confining pressure or pre-tightening force. And the grouting materials used in the test are different from the actual working conditions of the anchor rod, so it is difficult to accurately simulate the field mechanical environment of the surrounding rock mass and the anchor rod. As a result, the results obtained when analyzing the load transfer characteristics of anchors are often deviated from the engineering practice. Therefore, a large scale anchoring and drawing experiment system has been designed in the laboratory. The application of FBG force-measuring anchor rod, surrounding rock pressure, pre-tightening torque and new resin anchoring agent are taken into account. The axial force distribution characteristics of end anchoring and full-length Anchorage pre-tightening force are revealed.

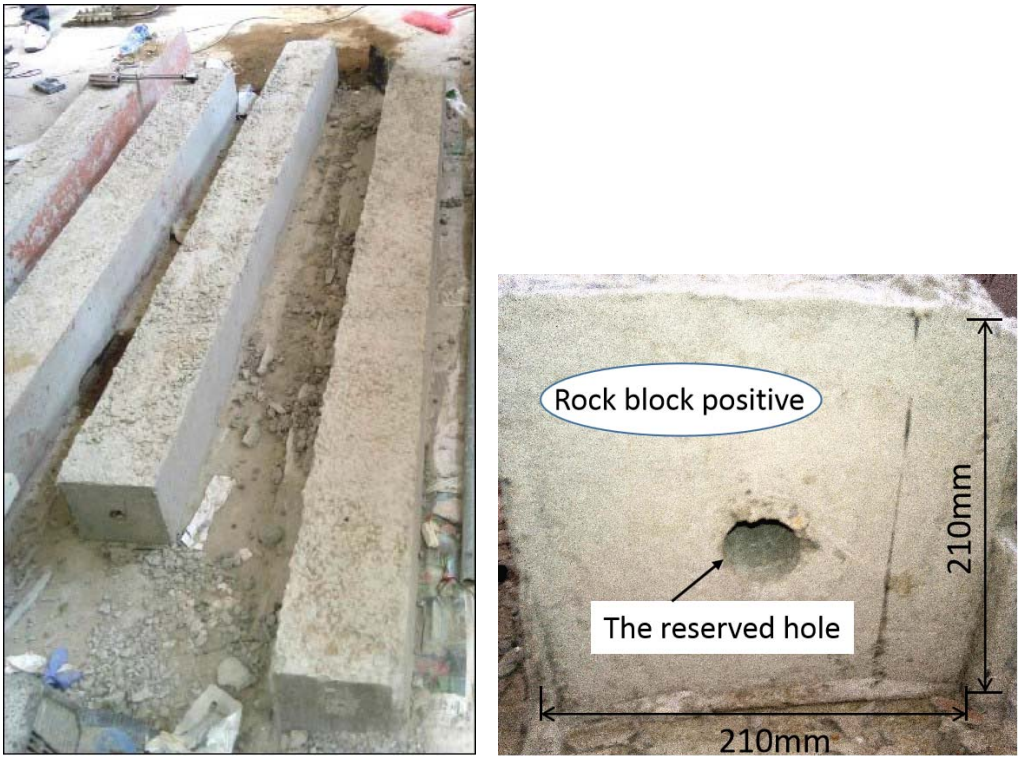

(a) (b)

Fig. 2. Surrounding rock specimen. (a) Overall picture of rock mass; (b) Cross section of rock specimen

2. Experimental Scheme Design

2.1. Experimental device and Preparation

The size of the surrounding rock specimen is 210 × 210 × 2500 mm, and the borehole with a diameter of 32 mm is reserved. The similar ratio of the experiment is 1:1. In Figure 1 (a) is the cross section of the surrounding rock and (b) is the Overall picture of surrounding rock mass. According to the physical and mechanical parameters of the surrounding rock of the roadway in the second level 62204 working face of Xinzhuangzi Coal Mine of Huainan Mining Group, the material ratio of the surrounding rock is calculated and simulated. The simulated samples were made of cement, river sand and stone with a grain size of about 5-7 mm, water content 175 kg, cement 461 kg, fine river sand 512 kg, gravel 1252 kg, in each cubic meter, the ratio of material is 0.38:1:1.11:2.72.

In the manufacturing process, a circular steel tube with a diameter of 32 mm is reserved in the middle of the mould. The mixing material is poured into the mold and vibrated evenly with the concrete vibrating rod. After the mixture solidifies for two hours, the pre-embedded circular steel tube is extracted and the concrete is maintained. The maximum uniaxial compressive strength of

the model material is 14.9 MPa, the elastic modulus E is 30.426 GPa, and the shear modulus is 12.016 GPa, which is basically equivalent to the main physical parameters of the surrounding rock.

The steel bolt with a total length of 2.5m and the diameter of 22 mm, the yield strength is 330 MPa, the tensile strength is 507 MPa, the elastic modulus is 201.7 GPa and the Poisson's ratio is 0.31. The continuous rolling thread is rolled at the whole length of the rod body, and the prestressed end gasket and ball head nut are arranged at the fastening end. Z2360 ordinary anchorage agent is used for anchorage at the end, one anchorage agent of 60 cm length is used for each reserved borehole, and a new resin anchorage agent Z2560 is used for full-length anchorage, and four anchorage agents are used for each borehole. The main parameters of the two anchoring agents are shown in Table 1.

TABLE 1

Main parameters of the two anchoring agents

Anchorage agent	Diameter /mm	Consistency /mm	Gel time /s	Elastic modulus /GPa	Poisson's ratio
Z2360	23	39	90~180	17	0.25
Z2560	25	46	120~180	22	0.28

Surrounding rock pressure loading is carried out on a three-dimensional similar simulation test stand with a dimension of 2 m × 1.2 m × 2 m, as shown in Figure 3. There are welded thick roof beams on the top and three wide channel steels on both sides as pillars, which can be used as supporting points to exert surrounding rock pressure.YBZ2*2-50A manual hydraulic jack is

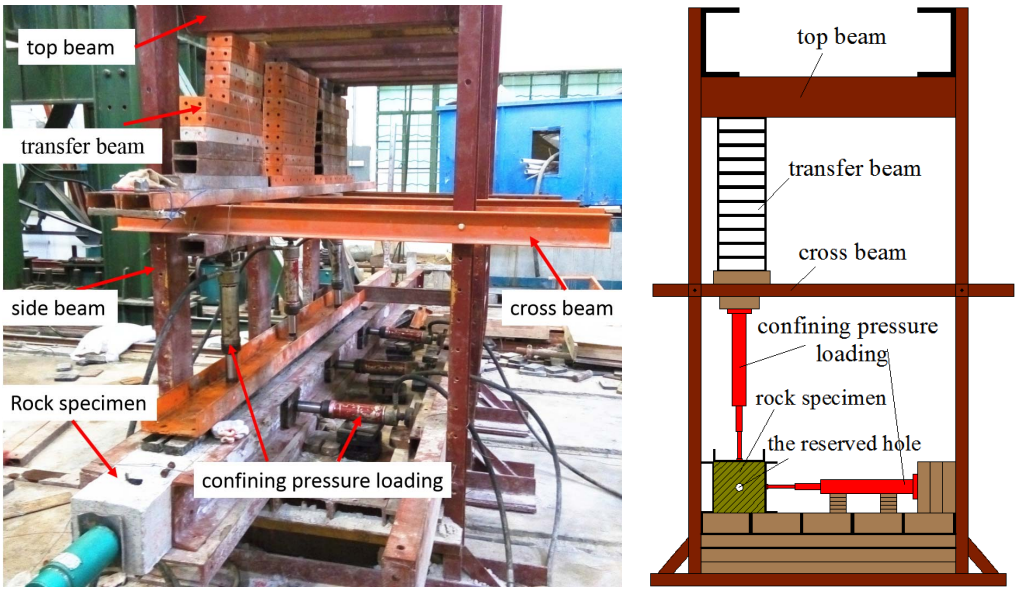

(a) (b)

Fig. 3. Large scale Anchorage system. (a) Anchor system scene; (b) Frontal view of experimental platform

used for pressurization. It is divided into two loops with three jacks in each loop and loaded with vertical and horizontal pressure, respectively.

In view of the fact that the optical fiber is made of glass, which is easy to break. In order to keep the optical fiber from being affected in the process of anchoring the bolt, and to sensitively feel the deformation of the bolt during the drawing process, a shallow groove of 1 mm depth, 1 mm width and 2460 mm length is cut along the bolt shank longitudinally on the lathe, and a groove of 2 mm depth and 2 mm width is cut at the end of the bolt thread to place the protective optical cable. The size and effect of the anchor groove are shown in Figure 4.

The fiber type is SMG.652b, the wavelength range is 1520~1580 nm, the fiber diameter is 0.18mm, the working temperature is between –20~80℃, the measurement accuracy is <1% F·S, and the pressure sensitivity of the fiber grating is 0.0141 nm/kN, the temperature sensitivity is 0.0111 nm/℃, fiber optic force measuring anchor is encapsulated with epoxy resin. The main technical parameters of fiber grating force measuring anchor are shown in Table 2. According to the physical and mechanical parameters of the anchor and the fiber, the selected fiber sensor can be selected to meet the detection requirements.

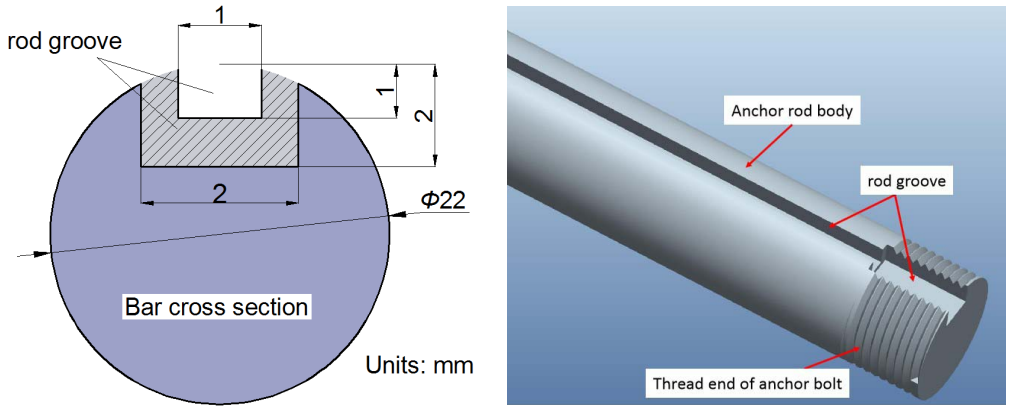

(a) (b)

Fig. 4. Anchor rod groove. (a) bolt slot cutting specification; (b) slot bolt integral diagram

TABLE 2

Main technical parameters of fiber grating force measuring anchor

Fiber type	Measurement accuracy	Diameter of Fiber /mm	Operating temperature /℃	Wavelength range /nm	Package form	Pressure sensitivity /nm/kN	Temperature sensitivity /pm/℃
SMG.652b	<1% F·S	0.18	–20~80	1520~1580	Epoxy resin	0.0141	0.0111

Six grating measuring points are arranged on the grating fiber. The distance between each measuring point and the bolt thread end is shown in Figure 5.

A 60 cm long anchoring agent was placed in the borehole for end anchorage, four Z2560 new resin anchoring agents were placed in the borehole for full-length anchorage. Then anchored

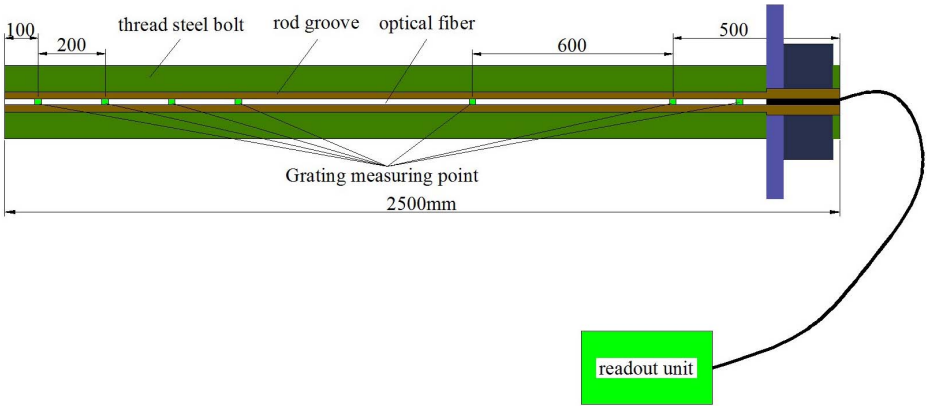

Fig. 5. Layout of anchor points

with anchor drill, what we should pay attention to is: before anchoring, the protective fiber optic cable needs to be coiled up and fixed at the end of the anchor rod with adhesive tape to prevent it from winding and breaking.

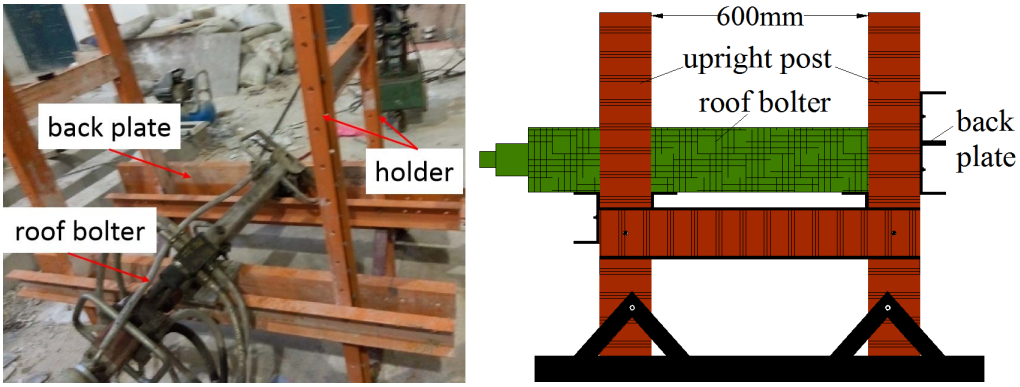

(a) (b)

Fig. 6. Overall platform of anchor drill. (a) Anchor drill; (b) Side view of anchor platform

2.2. Drawing Experiment

The loading pressure of surrounding rock was set according to the actual measured pressure. The vertical pressure is 10 MPa, the horizontal pressure is 13 MPa, and the preloading torque is 200 Nm. The room temperature is controlled by central air conditioning at 27 degrees. Considering the short time of experiment, the absolute value of wavelength drift caused by temperature is less than 2 pm, according to a set of experiments, so the wavelength drift caused by temperature change is ignored. During drawing, the tensiometer is pressurized manually, and the data are recorded by the FBG demodulator with a constant gradient pressure of 2 MPa each time.

3. Results and Analysis

3.1. Analysis of end anchored bolt

Wavelength values of six grating measuring points on the rod body are recorded, using the relationship between fiber grating wavelength variation and rod strain:

$$\varepsilon_b = \zeta \cdot \varepsilon_f = \zeta \cdot (P_i - P_0) \cdot \eta \cdot 1000 \tag{1}$$

The conversion coefficient η between the fiber drift and the corresponding strain provided by the manufacturer is 0.845, according to the research results of Chai et al. (2012). and the bond relationship between fiber layer, bond layer and anchor slot and three groups of calibration measurements, the transfer coefficient of Z2360 anchoring agent sticking naked fiber Bragg grating to slotted bolt ζ is 1.15, and that of Z2560 anchoring agent ζ is 1.12. P_0 is the initial wavelength, the wavelength of drawing force is 0 ; P_i is the wavelength of Drawing at i times; The strain values of the bolts at each measuring point can be obtained by substituting them, according to the relationship between axial force and strain of the bolts in the elastic range:

$$P(x) = E_b \cdot A_b \cdot \varepsilon_b \tag{2}$$

According to formula (2), the axial force distribution of anchor bar under different load conditions is obtained. The axial force of anchor rod corresponding to different drawing forces, under the condition of vertical pressure of 10 MPa and horizontal pressure of 13 MPa, is shown in Figure 7.

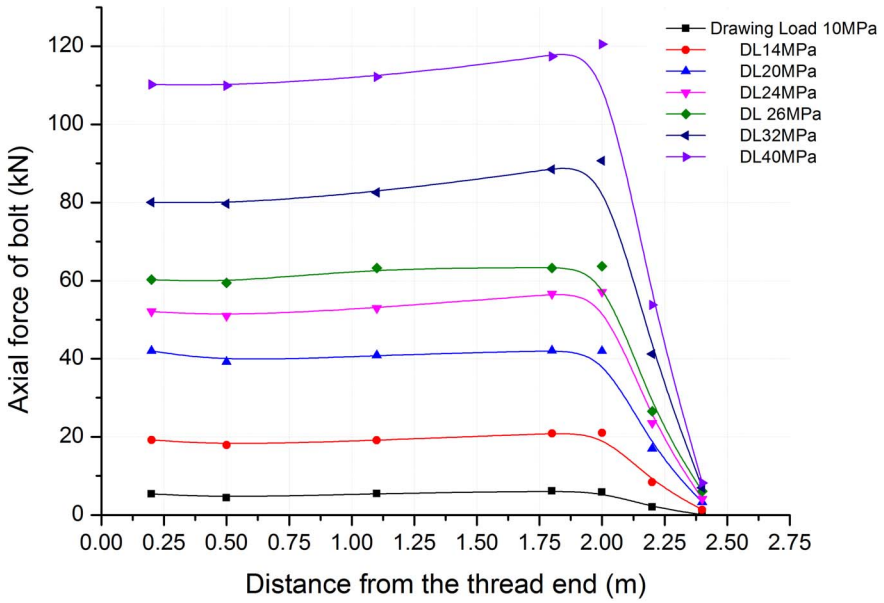

Fig. 7. Axial force variation of anchor rod

The force distribution law of anchoring section and free section of anchor rod can be obtained from the graph:

(1) The axial force of the anchorage part changes approximately linear, and the axial force in the middle of the anchorage section is slightly smaller than that in the linear trend with the increase of pulling force .
(2) The axial force of the free section changes linearly, and its value is equal to the maximum axial force of the anchoring section.
(3) The axial force increases slowly and the value of axial force is very small at the depth of 10 cm from the end of the bolt, because of the greater cohesion and friction between the bolt and the slurry.

3.2. Analysis of full length anchored bolt

The axial force distribution of anchored bolt under different load conditions can be obtained. The change of axial force of anchor bolt under different drawing force is shown in Figure 8.

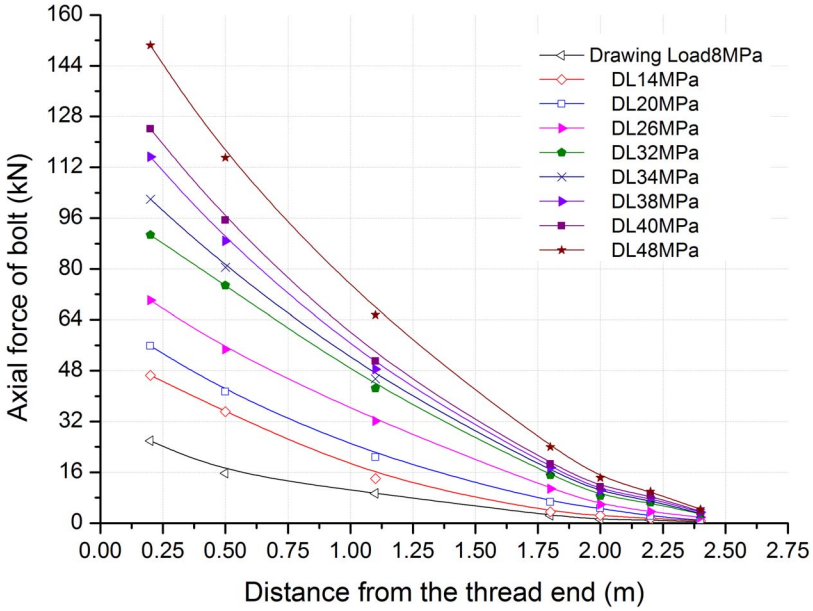

Fig. 8. Axial force variation of full length anchored bolt

(1) The axial force of full length anchored bolt decreases with the increase of anchorage depth;
(2) The axial force distribution is mainly concentrated in the anchorage zone from anchor thread section 0.2 m to 1.75 m position, which takes up about 3/5 of the length of the bolt and has a high slope and axial force value. The length from 1.75 m to anchor ends is about 2/5 of the length of the bolt, the axial force decreases slowly, and the axial force value is low;
(3) The axial force of the bolt varies little at the end of the anchoring section.

3.3. Comparison of two Anchorage modes

The difference between full-length Anchorage and end Anchorage is that the full-length Anchorage whole body is in contact with anchoring agent and surrounding rock, but the end Anchorage bolt is only partially in contact with Anchorage. So the transfer of pulling force is very different. Therefore, the axial force distribution of the full length anchor rod and the end anchor rod body is shown in the following figure by comparing the axial force distribution under different drawing forces.

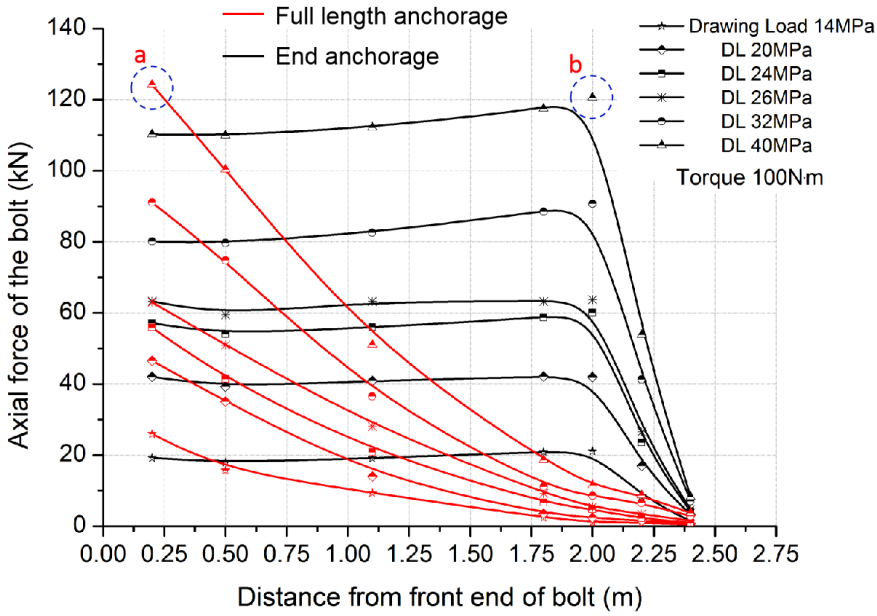

Fig. 9. Comparison of end Anchorage and Full-length Anchorage

The Figure 9 shows that the intermediate axial force of the end Anchorage section is lower than the average value of the section, and has the characteristics of concave, and the full-length anchoring is more obvious, similar to the hyperbolic distribution. Point a is the largest point of axial force in the full-length anchoring area, and point b is the maximum value of axial force at the end of anchoring. The maximum axial force at the anchoring end of the two kinds of anchoring modes is almost equal to that of the two kinds of anchoring modes, taking the maximum axial force of the two kinds of anchoring methods. The specific values are shown in Table 3.

The maximum axial force of anchor rod less than 1/4 times is defined as the low stress zone, and the maximum axial force greater than 3/4 times is defined as the high stress region of anchor rod. Calculation result shows that the average length of the low stress region of full-length Anchorage is 1.55 m to 2.5m, the ratio is 39.6%, The average length of high stress region is 0.1 m (0-0.1m is thread end) to 0.52 m, the percentage is 17.5%; The average length of the low stress zone at the end Anchorage is 2.28 m to 2.5 m, the proportion is 9.1%, and the average length of the high stress zone is 0.1 m to 2.1 m, accounting for 83.3%.

TABLE 3

Maximum axial force corresponding to drawing force

Anchoring mode	Drawing force/MPa					
	14 MPa	20 MPa	24 MPa	26 MPa	32 MPa	40 MPa
	Maximum axial force value /kN					
End	21.04	42.08	58.6	63.7	90.69	120.05
Full-length	25.94	46.52	55.8	63.02	91.08	120.14

Therefore, only for the bearing capacity of anchor rod, the main bearing range of two kinds of anchoring modes can be obtained. The main bearing range of full-length anchoring is near the thread end of anchor rod, the ratio of high stress range is only 17.5%. The main bearing range of end Anchorage is larger. The proportion of high stress range reaches 83.3% and the high stress range extends to the deep surrounding rock, which is more advantageous to play the role of anchor rod. These are consistent with the findings of Wang Hongtao (2014) Phillips S.H.E. et al. (1970).The use of full-length anchoring in broken rock mass can increase the bond property of anchoring agent and surrounding rock, and make it form integrity better. When the integrity of surrounding rock is better, it is more advantageous to reduce anchoring length of anchor rod to transfer axial force.

4. Field Test

4.1. Roadway geology

The 62204 fully mechanized coal face of Xinzhuangzi coal mine, Huainan City, China, with a elevation of –698 m ~ –805 m and a length of opening and cutting hole is 159 m. B4 coal seam is a medium thick coal seam with complicated structure. The average thickness of coal seam is about 3.4 m. The coal seam has simple structure and stable occurrence. The coal seam roof and floor are shown in Table 4.

TABLE 4

Coal seam roof and floor

Roof and floor	Rock property	Thickness (m)	Physical and mechanical properties		
			Compression strength /MPa	Tensile strength /MPa	Poisson ratio
main roof	Medium grain sandstone	3.5-4.0	25.32	1.52	0.31
immediate roof	Sandy mudstone	4.0-6.0	19.75	1.23	0.25
Direct bottom	Sandy mudstone	1.0-3.0	18.13	1.2	0.23

4.2. Site arrangement

Through the installation of force measuring bolt on the side and roof of the roadway along the channel, under the influence of mining face, the surrounding rock of the roadway is deformed, and then the force of the bolt is produced, and the force of the bolt is monitored in combination with the optical fiber sensing system. Thus, the stress variation law of roadway surrounding rock can be monitored.

Fig. 10. Drill hole

Fig. 11. Monitoring data

Considering that the 62204 cut hole is not completely through, in order to realize the monitoring of the optical fiber test system as soon as possible, the test station is arranged in the transport channel of 15 m in front of the working face, and the three stations are arranged at intervals of about 10 m respectively. Set a temperature compensation station between the three stations of the roadway, use three grating points in series with the fiber grating force measuring anchor, the bolt is anchored with 1/5 roll of resin anchoring agent, the anchoring length is about 10 cm, the grating measuring point is not within the anchorage range and the outer end of the bolt is free, ensuring that the grating points are unaffected by stress. The station layout is shown in Figure 12.

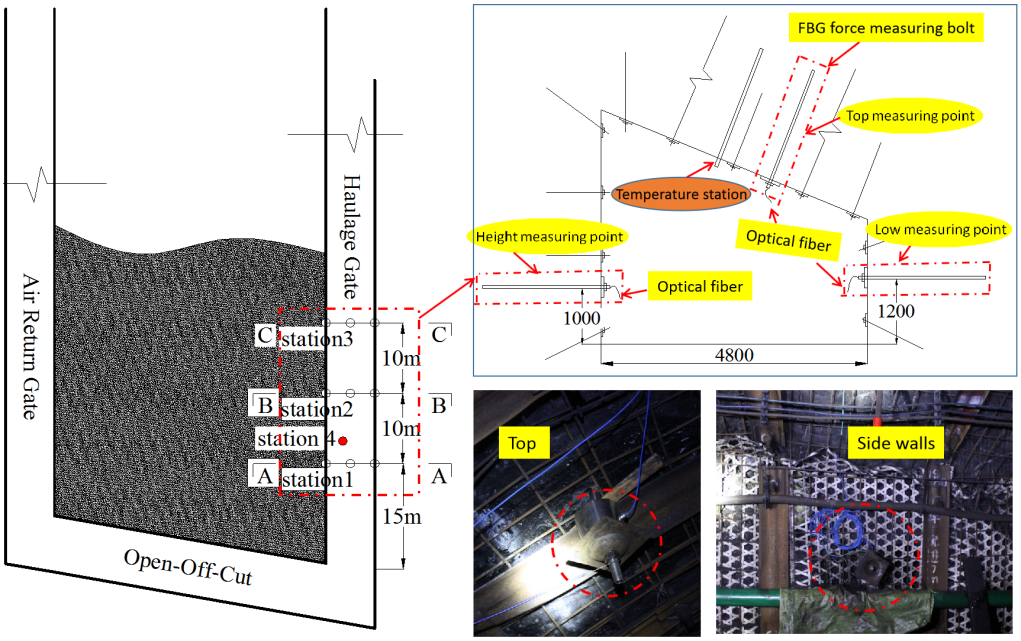

Fig. 12. Station layout

The three stations are located at A-A section B-B section and C-C section of roadway. Three measuring points are arranged in each station, which are located at the high side, the low side and the roof of the surrounding rock of the roadway, and one FBG force-measuring bolt is installed on each side and roof to detect the effect of the force-measuring anchor rod. The length of the FBG force-measuring anchor rod for end Anchorage is 2.5 m, and the five measuring points are located at 0.1 m, 0.3 m, 0.5 m, 0.6 m and 1.0 m from the front end of the anchor rod respectively. An anchorage agent roll are placed in the Anchorage hole, each of which is 60 cm long, the first four measuring points are located in the Anchorage area.

When anchoring, the measuring wire of fiber exposed is wound around and fixed to the end of anchor rod to prevent the wire from winding and breaking in the process of high speed agitation of bolt drill.

After the installation of all the measuring points in the roadway, the data of the fiber grating are recorded for the first time as the initial value of the fiber grating. The stress change of surrounding rock in observation roadway began on March 8 and ended on April 24. And according to the data measured by the temperature station, eliminate the influence of temperature effect, the axial force of FBG end Anchorage rod and the sensitivity of anchor rod testing with surrounding rock pressure are monitored and analyzed. The data of force measurement by FBG at 1 / 2 / 3 station are collected and sorted. The axial force distribution of the bolt along the body is shown in the Figure 13.

The axial force of the anchor rod increases in the Anchorage section, and the maximum axial force of the free end bolt is basically equal to that of the Anchorage section.After the final penetrating work on the open hole in April, the first mining of the working face was carried out, and the change of the axial force of the anchor rod was detected by the station near the cut hole. The deformation monitoring of the roadway showed that the change of the axial force of the anchor rod was obviously increased. From April 15 to April 20, the deformation of the roof and floor and the movement of the two sides of the roadway increased to a certain extent, and the axial force of the bolt increased from about 80 kN to 130 kN. FBG bolt is sensitive to the pressure and deformation of roadway and can be applied to the monitoring of roadway pressure.

The experimental results of axial force transfer and field measurement are shown in Figure 14. The experimental results show that the stress value of the anchor rod fits well with the field measured value, which effectively reflects the actual stress state of the anchoring section of the anchor rod in the field. The rationality and correctness of the system are proved.

5. Conclusion

A full scale anchoring and drawing experimental system with surrounding rock pressure and pretension torque was designed in laboratory with a simple device. The mechanical characteristics of prestressed end Anchorage and full-length anchoring bolt were studied by the application of FBG test technology. The main results are as follows:

1) The axial force of the end Anchorage segment increases approximately linearly from the inside out, the axial force in the middle of the anchoring section is slightly smaller than that in the linear trend, and the axial force at the free end is almost unchanged.
2) The axial force distribution of the full-length anchor rod increases slowly from 2.5 to 1.75 m at the end of the bolt, and the axial force value is low, accounting for about

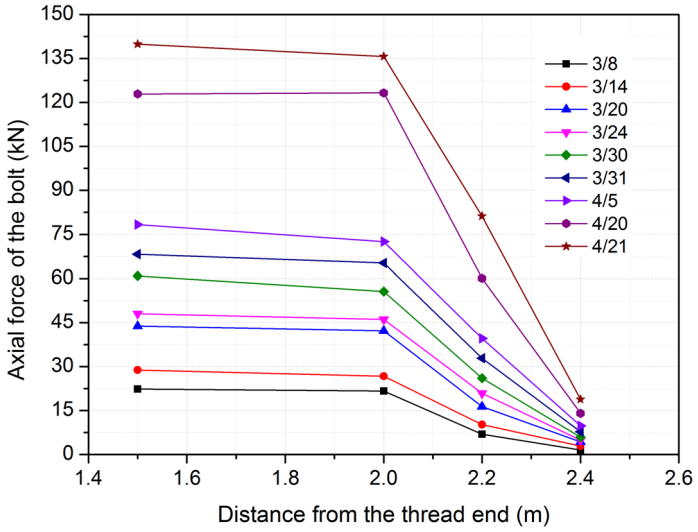

(a)

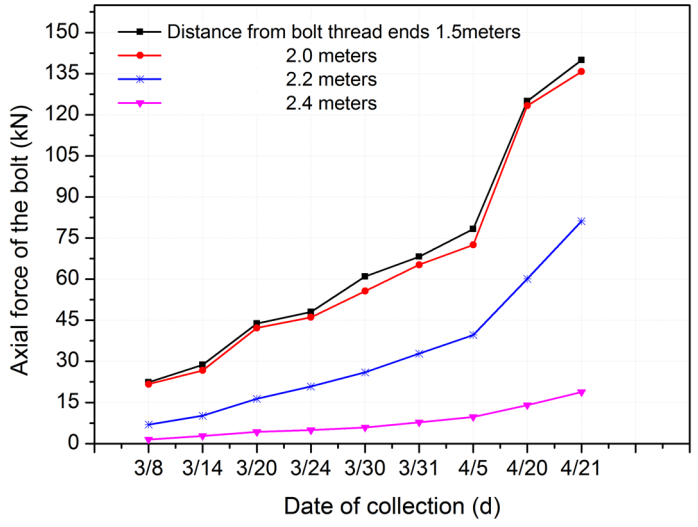

(b)

Fig. 13. Field Monitoring results of the bolt axial stress. (a) Variation of axial force of bolt with time; (b) Variation of Axial Force in different position of bolt

2 / 5 of the length of the bolt, and the axial force is high from 1.75 m to 0.2 m from the end of the bolt thread.

3) The high and low stress zone of two types of anchoring bolts are divided. The full length Anchorage high stress zone is located near the bolt thread end, the proportion is only 17.5%. The main bearing range of the end Anchorage is larger, the proportion of the high stress zone is 83.3%, and the depth of the high stress can be transferred more.

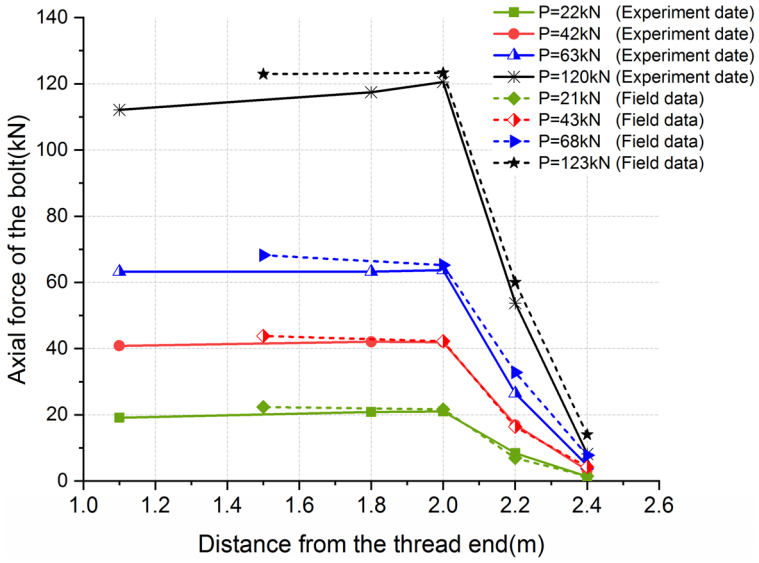

Fig.14. Comparisons between Field and experimental measured value of the bolt axial stress

4) Long-term field monitoring with fiber optic anchor rod shows that it is sensitive to the pressure and deformation of roadway and can be used to test the stress state of anchor rod. The experimental system of bolt drawing can describe the load transfer of anchor rod in situ well.

Acknowledgement

This work is supported by the National Natural Science Foundation of China (Nos. 51774009, 51074163, 51574228); Major Program of National Natural Science Foundation of China (No. 50834005, 51734009); the Graduate Innovation Fund Project of Jiangsu Province (No. CXZZ13_0924); Open Fund of State Key Laboratory for Geomechanics and Deep Underground Engineering (SKLGDUEK1409)

Author Contributions

Tuo Wang and Jucai Chang conceived and established the experimental system; GongPeng guided thesis writing; Wenbao Shi , Ning Li and Shixing Cheng analyzed the data; Tuo Wang wrote the paper.

References

Stillborg B., 1984. *Experimental investigation of steel cables for rock reinforcement in hard rock.* PhD thesis (Unpublished) Lulea University, Lulea .

Benmokrane B., Chennouf H.S., 1995. *MitriLaboratory evaluation of cement-based grouts and grouted rock anchors.* Int. J. Rock Mech. Min. Sci. **32**, 7, 633-642.

Chen J., Hagan P.C., Saydam S., 2016. *Load transfer behaviour of fully grouted cable bolts reinforced in weak rocks under tensile loading conditions*. Geotech. Test. J. **39**, 2, 252-263.

Chen J., Hagan P.C., Saydam S., 2017. *Sample diameter effect on bonding capacity of fully grouted cable bolts.* Tunn Undergr Space Technol. **68**, 238-243.

C.R. Windsor, A.G., 1993. *ThompsonRock reinforcement-technology, testing, design and evaluation JA Hudson* (Ed.). Comprehensive rock engineering, Pergamon Press, Oxford, p. 451-484.

Cai Y., Esaki T., Jiang Y., 2004. *An analytical model to predict axial load in grouted rock bolt for soft rock tunnelling.* Tunn. Undergr. Space Technol. **19**, 6, 607-618.

Chen J., Hagan P.C., Saydam S., 2016. *Load transfer behaviour of fully grouted cable bolts reinforced in weak rocks under tensile loading conditions.* Geotech. Test J. **39**, 2, 252-263.

Chai Jing, Zhao W.H. et al., 2012. *Pull out tests of figer Bragg grating sensor fitted bolts.* Journal of China University of Mining and Technology **41**, 5, 719-724.

Ren F.F., Yang Z.J., Chen J.F., Chen W.W., 2010. *An analytical analysis of the full-range behaviour of grouted rockbolts based on a tri-linear bond-slip model.* Constr. Build. Mater. **24**, 361-370.

Forbes B., Vlachopoulos N., Hyett Andrew J., Diederichs Mark S., 2017. *A new optical sensing technique for monitoring shear of rock bolts.* Tunn. Undergr. Space Technol. **66**, 34-46.

Gao F., Kang H., 2008. *Effect of pre-tensioned rock bolts on stress redistribution around a roadway – insight from numerical modeling.* J. China Univ. Min. Technol. **18**, 509-515.

Hillyer J., 2012. *Influence of installation method and resin properties on rock bolt performance in underground coal mines.* Undergraduate thesis. UOW, p. 1109.

Kang Hongpu, Wang Jinhua, Lin Jian, 2010. *Case studies of rock bolting in coal mine roadways*. Journal of Rock Mechanics and Engineering **29**, 04, 649-664.

Kang H., Lin J., Wu Y., 2009. *Development of high pretensioned and intensive supporting system and its application in coal mine roadways.* Proc. Earth Planet. Sci. **1**, 479-485.

Li CC., 2007. *A Practical problem with threaded rebar bolts in reinforcing largely deformed rock masses.* Rock Mechanics and Rock Engineering **40**, 5, 519-24.

Li L., Hagan, P.C., Saydam, S., Hebblewhite, B., 2016. *Shear resistance contribution of support systems in double shear tests.* Tun. Undergr. Space Technol. **56**, 168-175.

Li Chong, XU Jin-Hai., 2013. *The mechanical characteristics analysis of fully anchored pre-stressed bolts in coal mines.* Journal of Mining and Safety Engineering **30**, 2, 188-224.

López-Higuera J.M., Cobo L.R., Incera A.Q., Cobo A., 2011. *Fiber optic sensors in structural health monitoring.* Journal of Lightwave Technolog **29**, 4, 587-608.

Li Shucai, Wang Hongtao, Wang Qi et al., 2014. *Limit analysis of failuremechanism of prestressed anchor cable based on Hoek-Brown fail-ure criterion.* Rock and Soil Mechanics **35**, 2, 466-473.

Vlachopoulos N. et al., 2018. *Utilizing a novel fiber optic technology to capture the axial responses of fully grouted rock bolts.* Journal of Rock Mechanics and Geotechnical Engineering **10**, 02, 222-235.

Patrick H.J., 2000. *Self aligning bipolar bend transducer based on long period grating written in core fiber.* Electronics Lett. **36**, 21, 1763-1764.

Phillips S.H.E., 1970. *Factors affecting the design of anchorages in rock.* London: Cementation Research Ltd.

Stillborg B., 1986. *Professional Users Handbook for Rock Bolting.* Clausthal-Zellerfeld, Germany: Trans Tech Publications.

Wang Tuo, Chang Jucai etc., 2016. *Research on bolt-mesh-anchor support technology in deep mine with hard roof*. Coal Engineering 48, 07, 50-52.

Habel W.R., Krebber K., 2011. *Fiber-optic sensor applications in civil and geotechnical engineering Photon.* Sens. **1**, 3, 268-280.

Zhang Guihua, Chai Jing et al., 2014. *Study on stress distribution of bolt in pullout test based on FBG*. Journal of Mining and Safety Engineering **31**, 04, 635-639.